# Dominant patterns of AVHRR NDVI interannual variability over the Sahel and linkages with key climate signals (1982-2003)

Lionel Jarlan, Y. M. Tourre, Éric Mougin, N. Philippon, P. Mazzega

# Dominant patterns of AVHRR NDVI interannual variability over the Sahel and linkages with key climate signals (1982–2003)

L. Jarlan,[1] Y. M. Tourre,[2,3] E. Mougin,[1] N. Philippon,[1,4] and P. Mazzega[5]

Received 26 October 2004; revised 10 December 2004; accepted 19 January 2005; published 16 February 2005.

[1] The spatio-temporal evolution of Sahelian vegetation is analyzed using the Normalized Difference Vegetation Index (NDVI) obtained from the NOAA/AVHRR sensor (1982–2003). Dominant patterns are identified using rotated EOFs. While the first four modes are associated with specific bio-geo-climatic conditions in space, significant time scales are detected using a multi-tapers method. Three interannual time scales (~6.2-, 4.5- and 3.6-year) are present in the first and third NDVI modes over the western Sahel. A quasi-biennial time scale (~2.6-year) is present in second and fourth NDVI modes over the northeast Sahel. During summer, significant lagged correlations are found between the NDVI second (9-month lag) and third (10-month lag) modes, the meridional Atlantic Sea Surface Temperature (SST) gradient, and the zonal SST gradient in the Indian Ocean. Potential physical linkages and dynamics with known climate fluctuations are discussed. **Citation:** Jarlan, L., Y. M. Tourre, E. Mougin, N. Philippon, and P. Mazzega (2005), Dominant patterns of AVHRR NDVI interannual variability over the Sahel and linkages with key climate signals (1982–2003), *Geophys. Res. Lett.*, *32*, L04701, doi:10.1029/2004GL021841.

## 1. Introduction

[2] Vegetation density variability over the Sahel depends on local rainfall variability [*Le Houérou*, 1989]. The latter is governed by West African Monsoon (WAM) dynamics, and spans over a large range of spatio-temporal scales [*Le Barbé et al.*, 2002]. Sea surface temperature (SST) anomalies are known to modulate Sahelian rainfall [e.g., *Palmer*, 1986; *Fontaine and Janicot*, 1996]. Inversely, vegetation density modifies the water and energy fluxes at the soil-vegetation-atmosphere interface, and thus feedbacks on WAM circulation and precipitation patterns [e.g., *Charney et al.*, 1977; *Zheng and Eltahir*, 1998].

[3] There is a growing need for detailed diagnostic studies on dominant spatio-temporal scales for vegetation variability. Some vegetation indices have been derived from the National Oceanic and Atmospheric Administration (NOAA) Advanced Very High Resolution Radiometer (AVHRR). As such, the Normalized Difference Vegetation Index (NDVI [*Tucker*, 1979]) data has already been used as an estimation of Sahelian vegetation biomass [*Tucker et al.*, 1985]. A study of the meridional movement of the Sahara-Sahel boundary [*Nicholson et al.*, 1998], and more recently a study of vegetation density trends over Sahel [*Eklundh and Olsson*, 2003] also used that index. *Anyamba et al.* [2002] have shown that the Pacific El Niño Southern Oscillation (ENSO) impacts vegetation density variability over east and south Africa. *Los et al.* [2001] studied the joint interannual variability between land surface vegetation, temperature, SST and precipitation on a global basis.

[4] The main objective here is to get a better understanding on the interannual variability of vegetation density with an emphasis on the Sahel region (1982–present), as a signature of WAM variability, possibly linked with known global and regional climate/environmental fluctuations. To that purpose, simple NDVI spatio-temporal patterns are extracted from complex geophysical signal. Indeed, NDVI represents an integrated measure of climate, soil, and vegetation variability. The possible linkages and mechanisms between the variability of the NDVI with key climate signals in the Atlantic and Indian oceans are discussed. This work is part of the African Monsoon Multidisciplinary Analysis project.

## 2. Data and Methods

[5] Vegetation density variability using NDVI, takes advantages of spectral response difference of chlorophyll-loaded vegetal tissues between the red and infra-red channels. Typical NDVI values range between 0 and 1 for vegetated areas. The higher the NDVI value, the higher the green vegetation density.

[6] The NDVI data set used in this study is processed by the Global Inventory Monitoring and Modeling Studies (GIMMS) at NASA. The time series are from five sensors: NOAA-7, -9, -11, -14 and -16. The most recent NDVI data set (version 3, with NOAA-16 calibration, August 2003) is used. The index is corrected for sensor degradation [*Los*, 1998] and slight differences between orbiting satellites (changes of Sun Zenith Angle). The GIMMS data is also corrected from the effects of stratospheric aerosols. Finally, data acquired by NOAA-11 (end of 1994) and NOAA-14 during 2000 (contaminated by sensors degradation) have been replaced by data from NOAA-9 and NOAA-16. The non-vegetation effects are minimized by synthesizing NDVI values, using a maximum value compositing procedure, following *Holben* [1986]. Several recent studies have checked the reliability of this NDVI data set [*Kaufmann et al.*, 2000; *Zhou et al.*, 2001; *Slayback et al.*, 2003]. Neither significant discontinuities and/or linear trends from satellite switching, nor strong effects of volcanic aerosols were found. The data set used here is from January 1982 to December 2003. Data is from 8km pixel at 10-day time steps. It is

[1]Centre d'Etudes Spatiales de la Biosphère, Toulouse, France.
[2]Médias-France, Centre National d'Etudes Spatiales, Toulouse, France.
[3]Lamont-Doherty Earth Observatory of Columbia University, Palisades, New York, USA.
[4]Centre de Recherches en Climatologie, Dijon, France.
[5]Laboratoire d'Etudes en Geophysique et Océanographie Spatiales, Toulouse, France.


0094-8276/05/2004GL021841

available from the Africa Data Dissemination Service at the following URL: http://igskmncnwb015.cr.usgs.gov/adds/.

[7] A temporal filter is applied to remove remaining cloud contaminated data. True detection of the signal is obtained by comparing the NDVI value at time t, or NDVI(t), with the mean of its two surrounding values NDVI(t − 1) and NDVI(t + 1), respectively. If NDVI(t) differs from this value from ±30%, it is replaced. Data are then averaged over three 10-day periods (one month). Monthly data is 'upscaled' using a 6 * 6 pixel averaging window, yielding a final resolution of 48 × 48 $km^2$. Seasonality and trend are removed from each grid-point time series before standardization. The studied area is the 'Sahel window' (12°N/18°N–18°W/18°E).

[8] The spatio-temporal structures and patterns of NDVI are obtained through rotated EOF procedure (Varimax criterion, after *Richman* [1986]), to eliminate possible overlap of eigenvalues sampling errors, and to isolate regional NDVI patterns (i.e., maximize local variance explained). The 11 modes retained for rotation explain 80% of total variance.

[9] To isolate significant time scales associated with vegetation density variability, the multi-tapers spectral analysis method, or MTM [*Mann and Park*, 1994], is applied to the first four principal components. Three tapers are used for reasonable frequency resolution whilst providing sufficient degrees of freedom for signal/noise decomposition. Significance of results is tested against a red noise spectrum hypothesis.

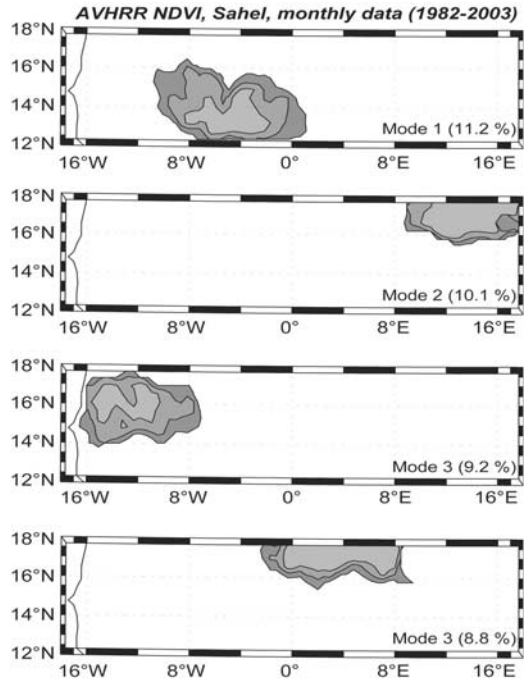


**Figure 1.** Loadings of rotated EOF of AVHRR NDVI over the 'Sahel window' (12°N/18°N and 18°W/18°E) during the period 1982–2003. Gray shadings represent the percentage of explained variance starting at 50% with incremental steps of 10%.

## 3. Results

[10] In Figure 1 spatial distribution of explained variance (up to 70%) for the first four rotated EOF modes retained (∼39% of the total variance), are displayed. The patterns are remarkably well distributed over the window and correspond to specific bio-geo-climatic domains. The first mode characterizes the inland Sahelian homogeneous bioclimatic conditions (between 12°N and 16°N, and between 11°W and 2E), inside the Niger Loop and under the influence of easterly waves and squall-lines [*Aspliden et al.*, 1976]. The second and fourth modes, to the north, represent Saharo-Sahelian conditions [*Le Houérou*, 1989]. They cover eastern Niger and western Chad (surrounded by the Tenere and the Tibesti mountains) and northern Niger (surrounded by the Adrar and Aïr mountains), respectively. The latter cover regions under orography-triggered squall-lines [*Aspliden et al.*, 1976]. The third mode extends from Senegal/southern Mauritania towards southern Mali, the region of the Senegal River Basin, the Ferlo, and of eastern Atlantic climate influence. It roughly corresponds to the specific west Sahelian rainfall domain of variability, highlighted by *Moron* [1994].

[11] Associated principal components (-PC- not shown here) highlight the strong interannual variability of vegetation conditions over the above areas. The well known dry 1984 and wet 1994 seasons [*Nicholson et al.*, 1996], characterized by homogeneous anomalies over the entire Sahel, appear clearly on the four PCs, whereas the 1999 rainy season doesn't exhibit such uniform behavior: it appears as wet as in 1994 for the first and fourth modes located around the center of the 'Sahelian window' but it is an average year for the second and third modes covering the eastern and western part of that window, respectively.

[12] Instead of PCs, the spectra for the first four modes are displayed in Figure 2, using MTM. Significant variances (90% to 99% levels) are found within two frequency bands: the narrow quasi-biennial band (or QB fluctuation, with peaks ∼2.6-year period for modes two and four), and the wider interannual band: three to eight years (or quasi-quadrennial QQ fluctuations, with peaks at ∼3.6- and 4.5-year periods for modes one and three). The 6.2-year peaks present in modes one and three have also been identified by *Mann and Park* [1996] when analyzing jointly global SST and sea level pressure, and by *Tourre and White* [2003], in the Indian Ocean. Care must be taken in the interpretation of the >6-year peaks due to the relative shortness of the NDVI time-series. Remarkably enough, most of the time scales identify here in NDVI variability, have already been highlighted from global [*Mann and Park*, 1996] and basin scales [*Tourre et al.*, 1999] analyses of climate fluctuations. *Los et al.* [2001] have also highlighted the 2.6- and 3.6-year periods with a different NDVI data set and over a shorter period (1982–1990) at the global scale.

[13] Further insight in possible associated climate dynamics is gained by correlating the NDVI modes to SSTs indices and gradients. The indices used, represent signatures of climate signals and SST variability in various part of the tropical oceans such as: "NINO3" in the equatorial Pacific ocean (150°W–90°W and 3°S–3°N, from OGP/NOAA), "ATL3" in the equatorial Atlantic ocean (20°W–GMT and 3°S–3°N, following *Servain* [1991]), and "IO1" in the equatorial Indian Ocean (80°E–95°E and 5°S–5°N, following *Tourre and White* [2003]). Time-series of meridional SST gradient in the tropical Atlantic (or TASI, following *Enfield et al.* [1999]) and zonal SST gradient in the tropical Indian

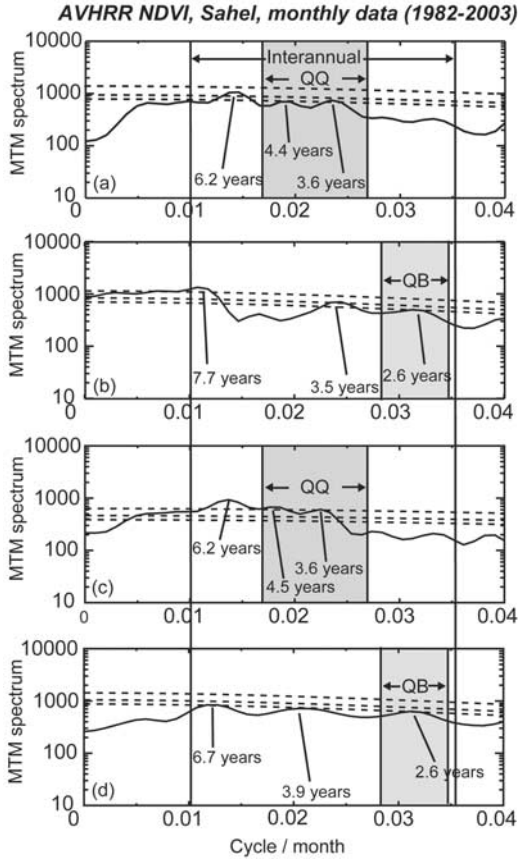


**Figure 2.** Truncated spectra of the first four principal components (2a to 2d) from the MTM method [*Mann and Park*, 1994]. Dotted lines correspond to 90%, 95% and 99% confidence levels (red noise hypothesis). Significant QQ/QB bands are found in modes one-three/two-four.

ocean (or IODMI, following *Saji et al.* [1999]) are also computed and correlated to NDVI PCs.

[14] Only significant correlations and associated lags are kept. In Table 1, only lagged correlations between the first four NDVI PCs averaged over July–August–September (JAS) and SST gradients in the Atlantic (meridional gradient, or TASI) and Indian (zonal gradient, or IODMI) oceans, also averaged over a three-month period, are displayed (from JAS-18 months to simultaneous correlation). Correlations are also calculated between SST gradients and a JAS Sahelian Rainfall Index from the Climate Prediction Center (CPC/NOAA) Merged Analyses Precipitation (CMAP) dataset, available at the following URL: http://www.cgd.ucar.edu/cas/guide/Data/xiearkin.html.

[15] The NDVI correlations with SST gradients are in general larger than correlations with local SST indices such as ATL3, and NINO3 mentioned above. This suggests that coupled climate dynamics over large oceanic areas is most important for modulating Sahelian land cover variability. This is discussed in the next section.

## 4. Discussion and Conclusion

[16] Significant QQ and QB signals are found in NDVI variability. The QQ fluctuations in modes 1 and 3, must be associated with signals identified by *Tourre et al.* [1999]. In their paper, an Atlantic 3.5-year climate fluctuation is shown to be linked with the global El Niño-Southern Oscillation phenomenon. An Atlantic 4.4-year signal is linked to local equatorial Atlantic interactions. The near-coastal area covered by the third NDVI mode is indeed under the direct influence of the eastern Atlantic ocean. Atlantic equatorial thermal conditions are then modified by the eastern Pacific thermal conditions associated with Pacific ENSO signatures. This is accomplished through modified zonal tropospheric circulation and ITCZ position over the eastern Atlantic [*Wang*, 2002], well before (9 to 18 months) precipitation over the Sahel during the following rainy season. QQ local maritime and deflected trade winds fluctuations lead to lower air temperature and larger rainfall amount with flooding of the Ferlo, adding to precipitation from the westward moving Sahelian squall-lines. The other QQ fluctuation (4.4-year period) must be linked to the local coupled fluctuations in the equatorial Atlantic [*Zebiak*, 1993; *Tourre et al.*, 1999]. Significant peaks of QB fluctuations are found over the inland 'trapped' Sahara-Sahelian second and fourth NDVI modes. These two modes are surrounded by mountains (south of the Djado Plateau and south of Hahaggar). Elevated areas are going to be influenced by QB fluctuations [*Weng*, 2003]. QB fluctuations have also a strong signature in the extreme Gulf of Guinea where the equatorial Atlantic ocean is alternatively warmer or colder (up to 2°C) every 16 months [*Konda et al.*, 1996]. Finally, the QB variability of the easternmost NDVI modes corroborates the role Indian ocean might play in Sahelian rainfall [*Tourre and White*, 2003], through additional advected water-vapor input. Both QQ and QB fluctuations presented above must then modulate atmospheric moisture conditions, rainfall for vegetation growth and, hence, NDVI variability.

[17] Significant lagged correlations (95% and 99% levels) of $r = -0.52$ ($-0.76$) (8-to-9 months lags) between TASI and NDVI Mode 1 (TASI and Ppt) mean that a negative TASI gradient during the Fall of year $t-1$, favors higher rainfall over the western Sahel during year t. TASI is known to modulate the latitudinal ITCZ position over West Africa [*Zheng and Eltahir*, 1998]. The lag must be linked to the memory effect in rain forest moisture content and land surface conditions identified by *Philippon and Fontaine* [2001]. Indeed wet Sahelian rainy seasons are often preceded by abnormally wet soils over the Sudan-Guinean belt during northern winter. Soil moisture anomalies hold during the Sahelian dry season and generate large moist static energy gradient inside the Niger Loop and over the West African continent, during the following rainy season. A significant lagged correlations (99% level) of $r = -0.65$ (9 months lags)

**Table 1.** Correlation Coefficient (and Significance Level of Correlation) Between NDVI July–August–September Modes and SST Gradients for the Atlantic (TASI) and Indian (IODMI) Oceans[a]

| | *Mode* 1 | *Mode* 2 | *Mode* 3 | *Mode* 4 | *Ppt Index* |
|---|---|---|---|---|---|
| *TASI* | $-0.52_{95\%}$ (9) | $-0.46_{90\%}$ (9) | $-0.65_{99\%}$ (9) | $-0.50_{95\%}$ (9) | $-0.76_{99\%}$ (8) |
| *IODMI* | $0.48_{90\%}$ (10) | $0.55_{99\%}$ (9) | $0.56_{99\%}$ (10) | 0.31 (9) | $0.58_{99\%}$ (10) |

[a]Time lead/lag in months are within parenthesis. Correlation between Sahelian rainfall anomaly index from CMAP (Ppt) and same SST indices/gradients is also presented.

between TASI and NDVI mode 3 means, as mentioned above, that low-frequency variability of the ITCZ position over the eastern Atlantic [*Tourre et al.*, 1999], must modulate precipitation amount and vegetation density over the Senegal River Basin. A significant correlation (99% level) between IODMI and Ppt of 0.58 (lag 10) is found. IODMI is also positively correlated (∼10-month lag) with the first three NDVI modes (0.48; 0.55; 0.56). This corroborates again the possible role played by additional water-vapor input from the Indian ocean, for Sahelian rainfall.

[18] Linkages between NDVI dominant patterns of variability over West Africa and dominant climate signals from neighbouring oceans, have been highlighted for the first time. Bio-geo-climatic conditions were isolated along with possible physical mechanisms: ITCZ location over the Atlantic and moisture input from the Indian ocean. Results should have applications in the agricultural and health sectors in the Sahel, in terms of decision-making for best prevention strategies and mitigation of climate impacts on population living there.

[19] **Acknowledgments.** Jarlan thanks the Centre National d' Etudes Spatiales for his post-doctoral fellowship. Tourre thanks MEDIAS-France for supporting his scientific activities. This work is also supported by the "Programme National de Tédétection Spatiale", the program "Terre – Ocean - Surface Continentale - Atmosphère, CNES" and the API "African Monsoon MultiDisciplinary Analysis (AMMA)". This is LDEO contribution # 6707.

## References

Anyamba, A., C. J. Tucker, and R. Mahoney (2002), From El Niño to La Niña: Vegetation response patterns over East and southern Africa during the 1997–2000 period, *J. Clim.*, *15*, 3096–3103.

Aspliden, C. I., Y. M. Tourre, and J. B. Sabine (1976), Some climatological aspects of West African disturbance lines during GATE, *Mon. Weather Rev.*, *8*, 1029–1035.

Charney, J., W. Quirk, S. Chow, and J. Kornfield (1977), A comparative study of the effects of albedo change on drought in semi-arid regions, *J. Atmos. Sci.*, *34*, 1366–1385.

Eklundh, L., and L. Olsson (2003), Vegetation index trends for the African Sahel 1982–1999, *Geophys. Res. Lett.*, *30*(8), 1430, doi:10.1029/2002GL016772.

Enfield, D. B., A. M. Mestas, D. A. Mayer, and L. Cid-Serrano (1999), How ubiquitous is the dipole relationship in tropical Atlantic sea surface temperatures?, *J. Geophys. Res.*, *104*, 7841–7848.

Fontaine, B., and S. Janicot (1996), Sea surface temperature fields associated with the West African rainfall anomaly types, *J. Clim.*, *9*, 2935–2940.

Holben, B. N. (1986), Characteristics of maximum-value composite images for temporal AVHRR data, *Int. J. Remote Sens.*, *7*, 1435–1445.

Kaufmann, R. K., L. Zhou, Y. Knyazikhin, N. Shabanov, R. Myneni, and C. J. Tucker (2000), Effect of orbital drift and sensor changes on the time series of AVHRR vegetation index data, *IEEE Trans. Geosci. Remote Sens.*, *38*, 2584–2597.

Konda, M., N. Imasato, and A. Shibata (1996), Analysis of the global relationship of biennial variation of sea surface temperature and air-sea heat flux using satellite data, *J. Oceanogr.*, *52*, 717–746.

Le Barbé, L., T. Lebel, and D. Tapsoba (2002), Rainfall variability in West Africa during the years 1950–90, *J. Clim.*, *15*, 187–202.

Le Houérou, H. N. (1989), *The Grazing Land Ecosystems of the African Sahel*, *Ecol. Stud.*, vol. 75, 282 pp., Springer, New York.

Los, S. (1998), Estimation of the ratio of sensor degradation between NOAA AVHRR channels 1 and 2 from monthly NDVI composites, *IEEE Trans. Geosci. Remote Sens.*, *36*, 206–213.

Los, S. O., G. J. Collatz, L. Bounoua, P. J. Sellers, and C. J. Tucker (2001), Global interannual variations in sea surface temperature and land surface vegetation, air temperature and precipitations, *J. Clim.*, *14*, 1535–1549.

Mann, M. E., and J. Park (1994), Global scale modes of surface temperature variability on interannual to century timescales, *J. Geophys. Res.*, *99*, 25,819–25,933.

Mann, M. E., and J. Park (1996), Joint spatio-temporal modes of surface temperature and sea level pressure variability in the Northern Hemisphere during the last century, *J. Clim.*, *9*, 2137–2162.

Moron, V. (1994), Guinean and Sahelian rainfall anomaly indices at annual and monthly scales (1933–1990), *Int. J. Clim.*, *14*, 325–341.

Nicholson, S. E., M. B. Ba, and J. Kim (1996), Rainfall in the Sahel during 1994, *Bull. Am. Meteorol. Soc.*, *9*, 1673–1676.

Nicholson, S. E., C. J. Tucker, and M. B. Ba (1998), Desertification, drought, and surface vegetation: An example from the West African Sahel, *Bull. Am. Meteorol. Soc.*, *79*, 815–829.

Palmer, T. N. (1986), Influence of the Atlantic, Pacific and Indian oceans on Sahel rainfall, *Nature*, *322*, 251–253.

Philippon, N., and B. Fontaine (2001), The relationship between the Sahelian and previous second Guinean rainy seasons: A monsoon regulation by soil wetness, *Ann. Geophys.*, *20*(4), 575–582.

Richman, M. B. (1986), Rotation of principal components, *J. Climatol.*, *6*, 293–335.

Saji, N. H., B. N. Goswami, P. N. Vinayachandran, and T. Yamagata (1999), A dipole mode in the tropical Indian Ocean, *Nature*, *401*, 360–363.

Servain, J. (1991), Simple climatic indices for the tropical Atlantic Ocean and some applications, *J. Geophys. Res.*, *96*, 15,137–15,146.

Slayback, D. A., J. E. Pinzon, S. O. Los, and C. Tucker (2003), Northern Hemisphere photosynthetic trends 1982–1999, *Global Change Biol.*, *9*, 1–15.

Tourre, Y. M., and W. B. White (2003), Patterns of coherent climate signals in the Indian Ocean during the 20th century, *Geophys. Res. Lett.*, *30*(23), 2224, doi:10.1029/2003GL018476.

Tourre, Y. M., B. Rajagopalan, and Y. Kushnir (1999), Dominant patterns of climate variability in the Atlantic Ocean during the last 136 years, *J. Clim.*, *12*, 2285–2299.

Tucker, C. J. (1979), Red and photographic infrared linear combinations for monitoring vegetation, *Remote Sens. Environ.*, *8*, 127–150.

Tucker, C. J., C. L. Vanpraet, M. J. Sharman, and G. Van Ittersum (1985), Satellite remote sensing of total herbaceous biomass production in the Senegalese Sahel: 1980–1984, *Remote Sens. Environ.*, *17*, 223–249.

Wang, C. (2002), Atlantic climate variability and its associated atmospheric circulation cells, *J. Clim.*, *15*, 1516–1536.

Weng, H. (2003), Impact of the 11-yr solar activity on the QBO in the climate system, *Adv. Atmos. Sci.*, *20*, 303–309.

Zebiak, S. (1993), Air-sea interaction in the equatorial Atlantic region, *J. Clim.*, *6*, 1567–1586.

Zheng, X., and E. A. B. Eltahir (1998), The role of vegetation in the dynamics of West Africa monsoon, *J. Clim.*, *11*, 2078–2096.

Zhou, L., C. J. Tucker, R. K. Kaufmann, D. Slayback, V. S. Shabanov, and R. B. Myneni (2001), Variations in northern vegetation activity inferred from satellite data of vegetation index during 1981 to 1999, *J. Geophys. Res.*, *106*, 20,069–20,083.

L. Jarlan, E. Mougin, and N. Philippon, Centre d'Etudes Spatiales de la Biosphère, 18 avenue Edouard Belin, F-31401 Toulouse Cedex 4, France. (lionel.jarlan@cesbio.cnes.fr)

P. Mazzega, Laboratoire d'Etudes en Geophysique et Océanographie Spatiales, 18 avenue Edouard Belin, F-31401 Toulouse Cedex 4, France.

Y. M. Tourre, Médias-France, CNES, Bpi 2102,18 avenue Edouard Belin, F-31401 Toulouse Cedex 9, France.